A 1.8 MeV K^+ Injector for the High Current Beam Transport Experiment

J. W. Kwan, F. M. Bieniosek, E. Henestroza, L. Prost and P. Seidl,

Lawrence Berkeley National Laboratory, Berkeley, CA, 94720 USA

Corresponding author: Joe W. Kwan
Lawrence Berkeley National Laboratory
Fusion Energy Research Program
1 Cyclotron Road, MS47-112
Berkeley, CA 94720 USA
Phone: 510 486-7631
Fax: 510 486-5392
e-mail: jwkwan@lbl.gov

SHORT TITLE: A 1.8 MeV K^+ Injector for HCX

Number of pages: 1 title page, 6 main body pages include reference, 1 figure caption page, and 5 figure pages, total is 13 pages

Number of tables: 0

Number of figures: 7

Paper submitted to 14th International Symposium on Heavy Ion Inertial Fusion, Moscow, Russia, May 26-31, 2002.

ABSTRACT

For the High Current Beam Transport Experiment (HCX) at LBNL, an injector is required to deliver up to 1.8 MV of 0.6 A K^+ beam with an emittance of ≈ 1 π-mm-mrad. We have successfully operated a 10-cm diameter surface ionization source together with an electrostatic quadrupole (ESQ) accelerator to meet these requirements. The pulse length is ≈ 4 μs, firing at once every 10-15 seconds. By optimizing the extraction diode and the ESQ voltages, we have obtained an output beam with good current density uniformity, except for a small increase near the beam edge. Characterization of the beam emerging from the injector included measurements of the intensity profile, beam imaging, and transverse phase space. These data along with comparison to computer simulations provide the knowledge base for designing and understanding future HCX experiments.

Keywords: HIF, injector, ion source, contact ionizer, aluminosilicate, ion gun, ESQ accelerator

1. INTRODUCTION

The High Current Beam Transport Experiment (HCX) at LBNL [1] requires a K^+ beam of up to 1.8 MV and current of 0.6 A with pulse length ≥ 4 μs. In order to study emittance growth, the initial beam emittance must be low at ≈1 π-mm-mrad. These specifications are typical for a single beam in a multiple beam injector system for heavy ion fusion drivers [2]. We have chosen to use the surface ionization source because it is by far the most developed concept that can deliver a single beam with the above required flat-top beam current, emittance, and stability. The injector was originally built for the earlier ILSE project [3] but has been modified to produce longer pulse length and improved beam optics.

2. INJECTOR DESIGN

A schematic diagram of the HCX injector is shown in Fig. 1. It is contained inside a pressure vessel (3.7-5.3 Atm.) that also houses the Marx generator and the high voltage dome with electronics inside (not shown). The injector consists of a 10-cm diameter (radius of curvature = 20.3 cm), hot surface ionization source followed by an extraction diode and an electrostatic quadrupole (ESQ) accelerator. Voltages to the various electrodes are obtained from a resistive divider. The Marx generator consists of 38 stages of a 2-section network that produces a flat-top voltage pulse. Recent modifications have extended the flat-top pulse length to 5.2 μs. The rise time of the Marx generator is a few μs, and the actual beam pulse on-off is controlled by a 5-μs voltage pulse applied to the extraction electrode (±80 kV) with a much faster rise time. Further discussion of the injector apparatus can be found in [4,5].

Previous experiments [3] with this injector have produced up to 0.8 A of K^+ ion beam at 2.0 MV by using a 17.0-cm diameter ion source; however the beam profile was found to be hollow with significant current density non-uniformity. The non-uniform density

could lead to further emittance growth and more difficult interpretation of experiments downstream. Our goal was to understand the cause of this aberration and to improve the beam optics in order to produce a uniform beam for the HCX experiments.

2.1 Ion Source and Extraction Diode

Alkali surface ionization ion sources emit 100-1000 times more singly charged ions (e.g., Cs^+ and K^+) than neutral atoms with a current density of a few mA/cm^2 when the source temperature is near 1100 °C [6]. Both K^+ contact ionizer sources and K^+ aluminosilicate sources have been used. The major advantages of these types of ion sources are the absence of gas flow, excellent beam current control and low emittance (due to low ion temperature and a solid emitter boundary).

Because the large aperture allows the electric field from the main diode to penetrate into the extraction region, the ion current (space charge limited emission) is controlled by both voltages applied to the main diode and to the extraction electrode. Spherical aberration occurs near the edge of the emitter and is more pronounced when the source radius is large. In order to improve the beam optics, we have reduced the ion source diameter from the ILSE version of 17.0 cm down to 10.0 cm, and modified the voltage distribution in the injector. This also reduced the beam current from 0.8 A to 0.6 A.

2.2 ESQ accelerator

ESQ beam transport can be effective at low ion velocity and it has the advantage of requiring only simple cylindrical electrodes. Furthermore, the ESQ can combine both functions of transverse focusing and longitudinal acceleration without increasing the number of electrodes. For these reasons, the ESQ accelerator is in the current baseline design for the injectors of HIF drivers, but there are some important issues affecting the design criteria.

Recent simulation studies show that aberrations from the "energy effect" in the ESQ part of the injector are decreased when the beam edge to electrode clearance is increased.

The energy effect is essentially a chromatic aberration due to varying kinetic energy arise from the beam potential, thus the effect is more pronounced for space charge dominated high current beams. The energy effect can cause an elliptical beam to become more rectangular whereas the image force can turn the beam spot into a diamond shape. A larger clearance between the beam edge and the electrodes also helps to reduce the influence of beam image multipoles. In the latest design, the beam emerging from the HCX injector has some imperfections but it is adequate for the HCX experiments.

Figure 2 is the result from simulation showing the evolution of beam envelopes and normalized rms emittance as the beam is accelerated from the diode exit to the end of the injector. In the HCX experiment, ion beam leaving the injector will enter into a matching section designed to reduce the beam area by 25 times and deliver a beam matched to the downstream transport lattice.

3. EXPERIMENTAL RESULTS

Due to scheduling deadlines, the machine was operated at the full 1.8 MV only briefly to confirm voltage holding. We experienced some irreproducible beam results earlier when the machine was operated near full voltage, and later found the problem to be due to plastic tubing collapsed under high pressure thus unpredictably changed the resistor divider setting. We have taken most emittance and profile data at 1.0 to 1.5 MV and checked the scaling characteristics. The beam current can be adjusted by varying the extraction voltage with corresponding changes in the optics.

3.1 Ion Source operation

Potassium was supplied to the contact ionizer source by dissociating K_2CO_3 that had been previously absorbed into the porous tungsten substrate. Each "doping" cycle lasted for about 25 hr. of useful run time spreading over ≈ 4 days before the beam current started to

decline. Due to such short life between doping cycles, the doped ionizer was not intended for long term use in HCX. It was used only to establish a reference data for the space-charge limited beam optics to compare the results with those obtained by the long-life aluminosilicate source. So far we have found no significant difference between the two types of surface ionization sources: both gave similar beam current and RMS envelope parameters.

In an earlier configuration (before the final optimization of the source radius of curvature and gap distances) and voltages, we measured the beam profile at the exit of the extraction diode just before the ESQ section. The data showed qualitative agreement with our EGUN simulation, both demonstrating the presence of a raised rim that can be attributed to the eventual development of a hollow beam profile [5]. By optimizing the extraction diode geometry and reducing the beam current, the spherical aberration was later improved and therefore the beam profile became more uniform. At present, there is a $\approx 20\%$ discrepancy between the measured beam current and that predict by computer simulation of the ion diode. A separate experiment will be conducted off-line (on a different test stand) to investigate this discrepancy.

3.2 Current density measurements

The beam current density profiles from slit scanner diagnostics in the x and y directions during the middle part of the pulse length, are depicted in Fig. 3. The measured profiles are compared with those obtained from PIC simulation (using WARP-3D). We found a 10-16% discrepancy in the rms envelope size, but the shapes have similar features. In addition, images of the beam spot were recorded by exposing Kapton films to about 100 beam pulses. We have done an exposure calibration indicating that the darkening of Kapton film was linear with beam current density in the 2-MV energy range [7].

Figure 4 shows the Kapton beam images before and after correcting the beam optics (decreasing the beam current to reduce spherical aberration and allowing more clearance

in the ESQ channel to avoid energy effect). Since the Kapton images were time-integrated over the entire pulse length, they also recorded (superimpose) the beam head and tail that were responsible for the complicated pattern inside the ellipses. Both simulations of the beam in the ESQ and the slit scanner diagnostics showed that the rms envelope of the beam head in the x-direction is significantly larger than that during the flat-top of the beam pulse. On the other hand, the tail is strongly focused due to the much lower current. The corresponding time-integrated images generated by computer simulations are shown Fig. 5. Projecting the current density from the kapton data resulted in beam profiles agreeing with those from the slit measurements (as in Fig. 3) after integrating over the whole beam pulse to include the head and tail dynamics.

3.3 Emittance measurements

Phase space measurements were also taken using double slits scanners at the end of the injector. Figure 6a shows the beam in x-x' phase space with a normalized emittance of 0.63 π-mm-mrad. For comparison, the phase-space distribution obtained from PIC simulation was processed through the emittance scanner software to produce Fig. 6b that has similar data resolution as measured data in Fig. 6c. Clearly, there is fair agreement in the shapes of the distribution between Fig. 6a and 6c but the rms envelope radii and angles differ significantly. Likewise the y-y' emittance comparison is depicted in Fig. 7a, 7b and 7c where the agreement is not as good. Since the self-consistent simulation (starting with space-charge-limited ion emission) gives 20% greater beam current than measured in the experiment, we should expect to see some differences between simulated emittance and the measured emittance.

4. CONCLUSION

For the HCX experiments, an injector has been constructed to deliver up to 1.8 MV, of 0.6 A K^+ beam with an emittance of ≈ 1 π-mm-mrad and with a pulse length of ≈ 4 μs. Both the contact-ionization and alumino-silicate sources produced nearly identical results

obtained in the first HCX section. The data showed qualitative agreement with computer simulation but a discrepancy in the beam current still remained to be resolved. This work is supported by the Office of Fusion Energy, US DOE under contract No. DE-AC03-76SF00098.

REFERENCES

[1] Seidl et al, see 2002 HIF symposium proceeding

[2] J.W. Kwan, et al, Nucl. Instrum. and Methods (A), 464, p379, (2001)

[3] S.S. Yu, et al, Proc. of Inter. Symp. on Heavy Ion Inertial Fusion, Princeton, New Jersey, Sept. 6-9, 1995, Fusion Engineering and Design 32-33, 309, (1996).

[4] F. M. Bieniosek, E. Henestroza, J.W. Kwan, L. Prost, and P. Seidl, Proc. Particle Accelerator Conf., Chicago, p2099 June, (2001),

[5] F. M. Bieniosek, E. Henestroza, and J.W. Kwan, Rev. Sci. Instrum, 73, p1042, (2002)

[6] J.W. Kwan, W.W. Chupp, and S. Eylon, Proc. Particle Accelerator Conf., Vancouver, p2755, May, (1997)

[7] F. M. Bieniosek, J.W. Kwan, L. Prost, and P. Seidl, to be published in Rev. Sci. Instrum. August, (2002).

FIGURE CAPTIONS

Fig. 1. Schematic diagram of the HCX injector.

Fig. 2. (a) Beam envelopes evolution, units are in m. (b) RMS emittance evolution, units are in m and π-mm-mrad.

Fig. 3. Beam profiles in the horizontal and vertical directions at 33.81 cm and 34.18 cm down stream of the injector exit respectively. Vertical scale is arbitrary, normalized PIC results to give same integration as the experimental data.

Fig. 4. Kapton images of beam at the injector exit, before and after optimizing the optics.

Fig. 5. Images obtained from time-dependent simulation, before and after optimizing the optics.

Fig. 6. X-X' emittance diagrams. (a) from simulation, (b) from simulation result processed through slit scanner software, (c) from slit scanner measurement. Contours are intensity levels at 10% steps.

Fig. 7. Y-Y' emittance diagrams correspond to those in Fig. 6 for X-X'.

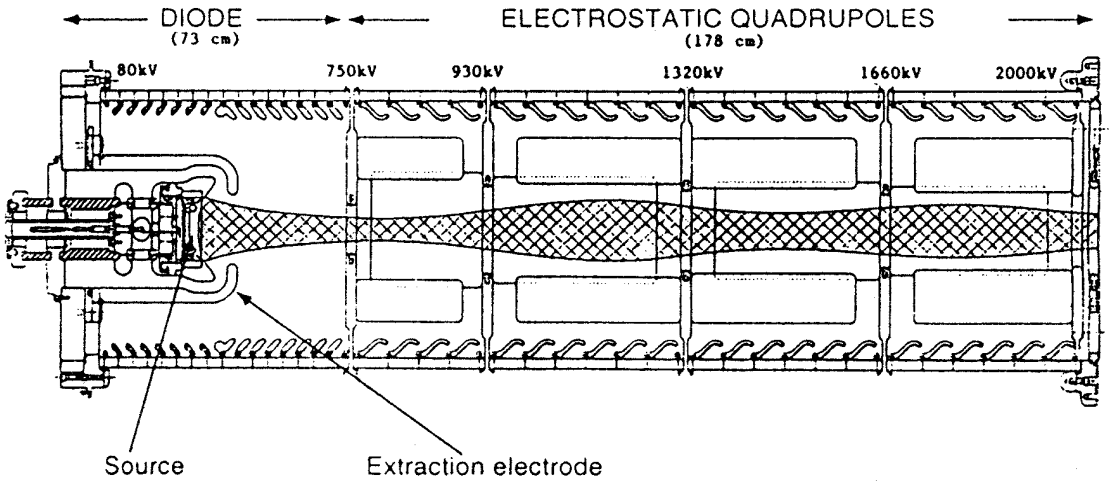

Fig. 1. Schematic diagram of the HCX injector.

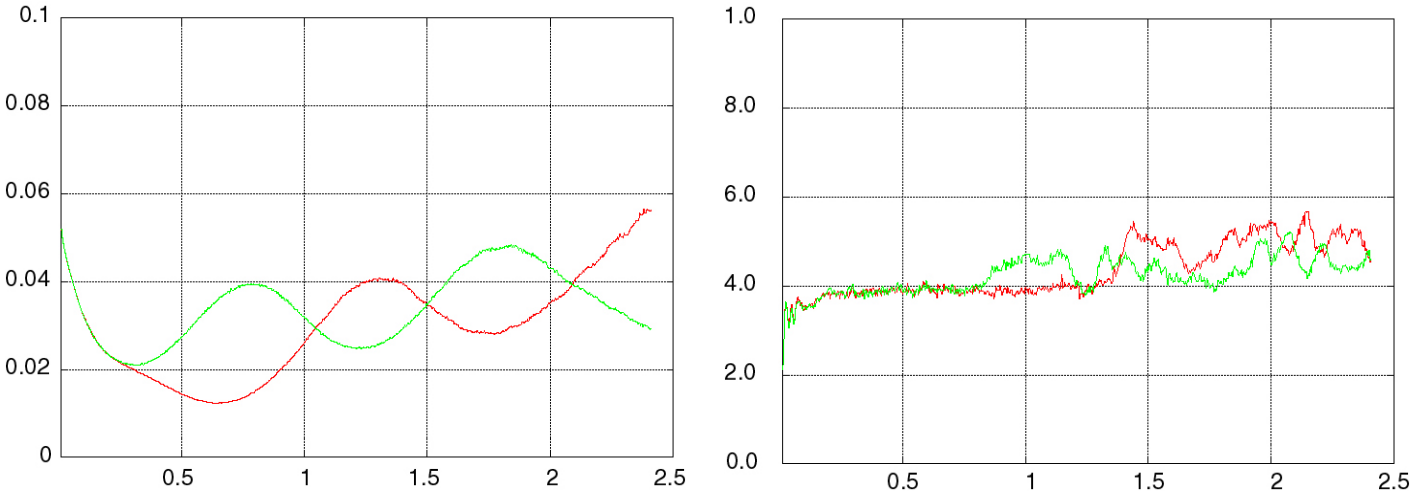

Fig. 2. (a) Beam envelopes evolution, units are in m. (b) RMS emittance evolution, units are in m and π-mm-mrad.

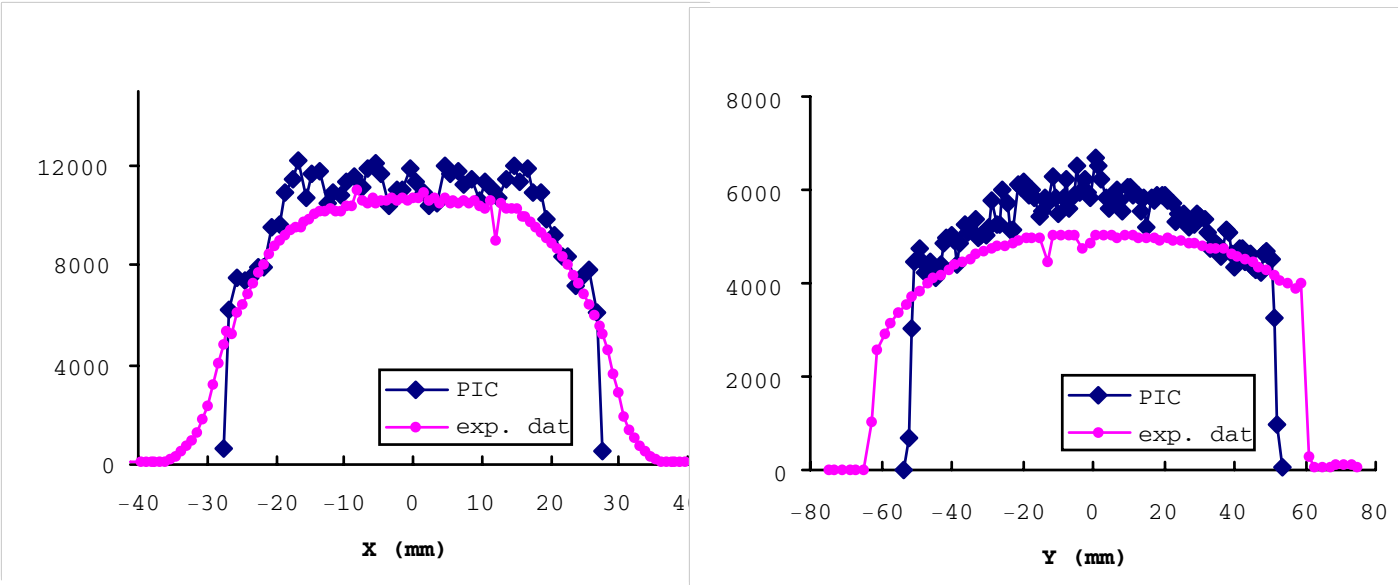

Fig. 3. Beam profiles in the horizontal and vertical directions at 33.81 cm and 34.18 cm down stream of the injector exit respectively. Vertical scale is arbitrary, normalized PIC results to give same integration as the experimental data.

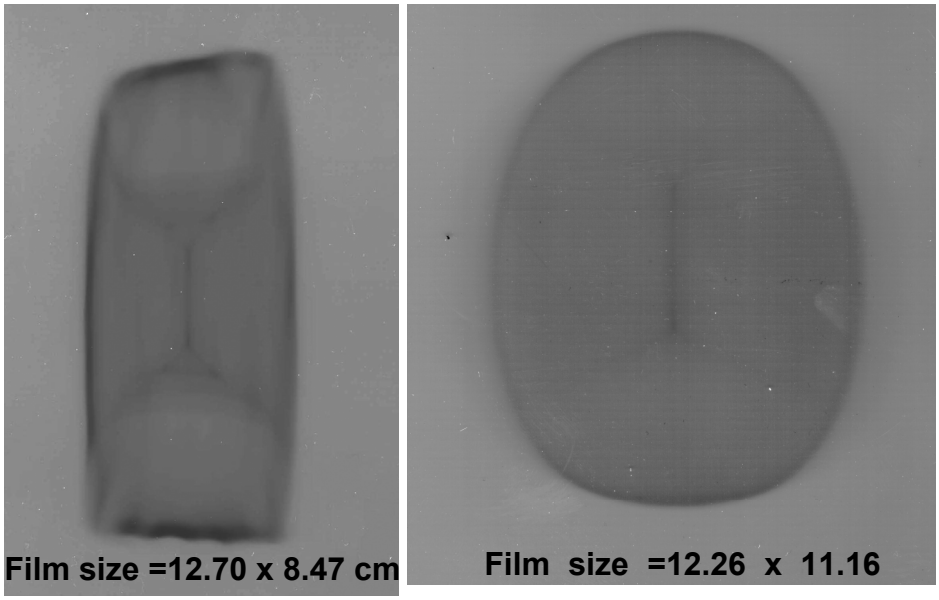

Fig. 4. Kapton images of beam at the injector exit, before and after optimizing the optics.

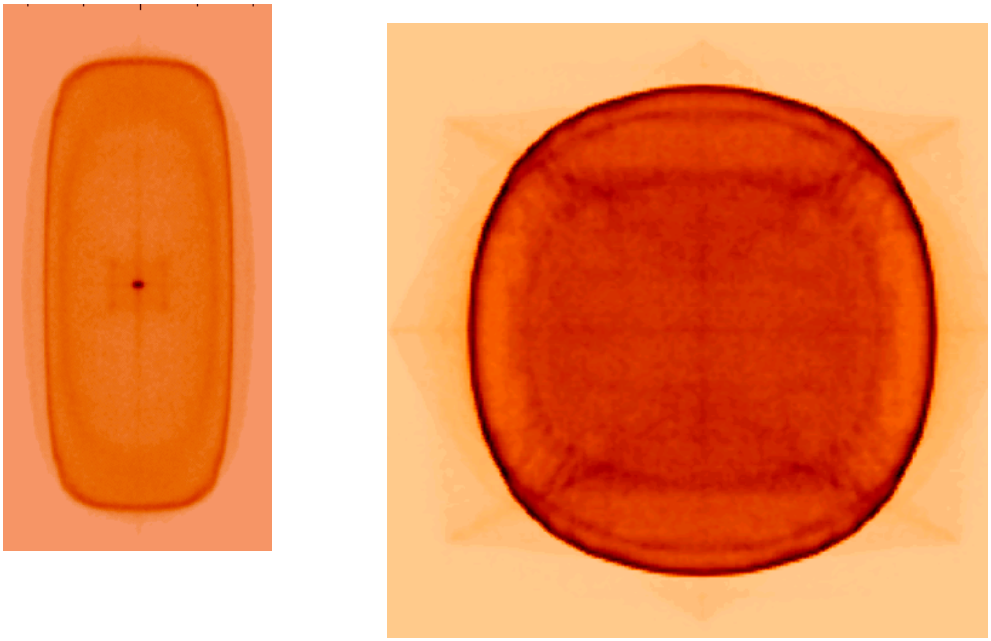

Fig. 5. Images obtained from time-dependent simulation, before and after optimizing the optics.

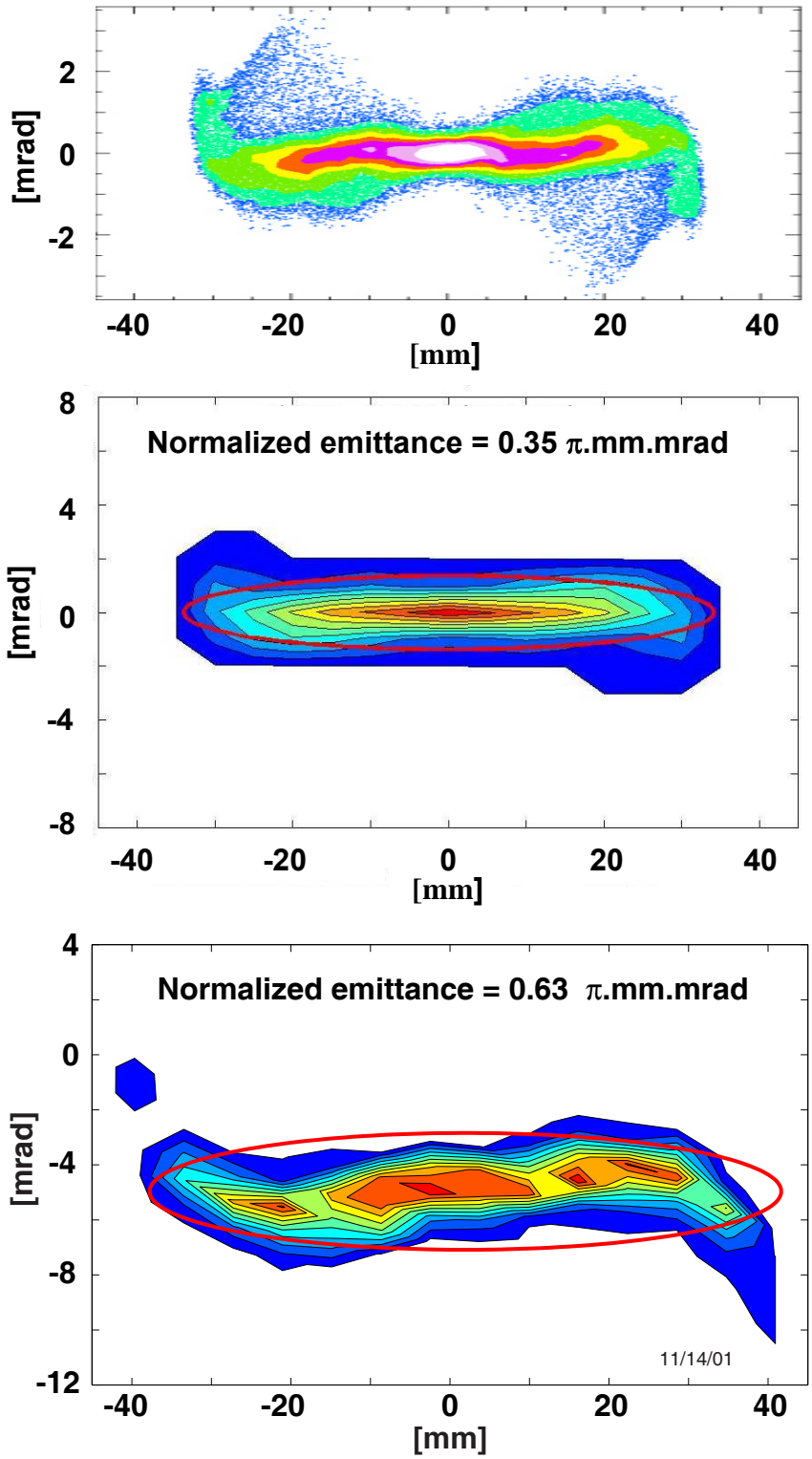

Fig. 6. X-X' emittance diagrams. (a) from simulation, (b) from simulation result processed through slit scanner software, (c) from slit scanner measurement. Contours are intensity levels at 10% steps.

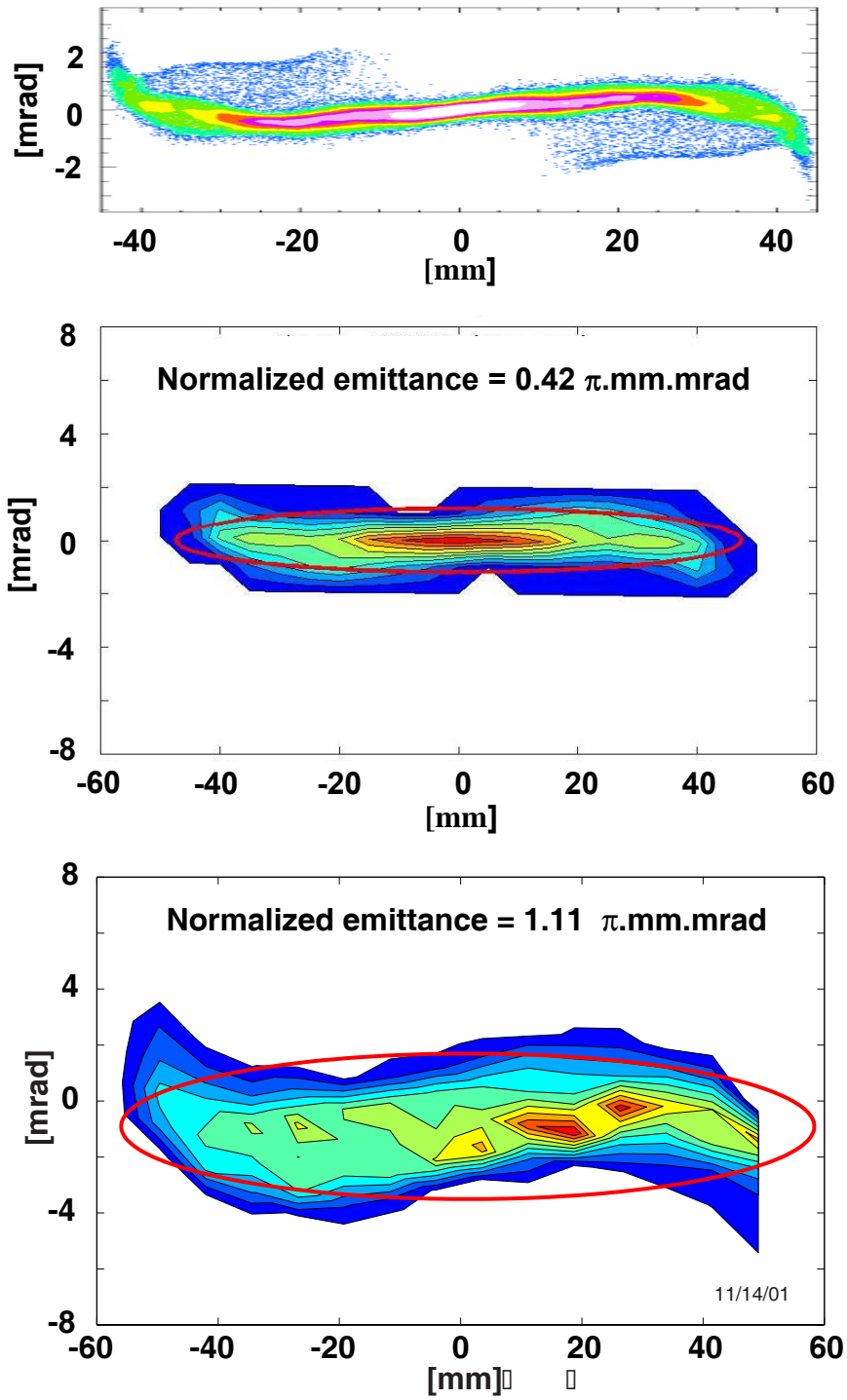

Fig. 7. Y-Y' emittance diagrams correspond to those in Fig. 6 for X-X'.